Heliyon 10 (2024) e34949

Contents lists available at ScienceDirect

Heliyon

journal homepage: www.cell.com/heliyon

Research article

MiR-338–5p, a novel metastasis-related miRNA, inhibits triple-negative breast cancer progression by targeting the ETS1/NOTCH1 axis

Wen-Jia Chen [a,b,1], Qian-Qian Ye [c,1], Hua-Tao Wu [d,1], Zheng Wu [a,b], Yang-Zheng Lan [a,b], Ze-Xuan Fang [a,b], Wen-Ting Lin [e], Jing Liu [a,b,*]

[a] The Breast Center, Cancer Hospital of Shantou University Medical College, Shantou, 515041, China
[b] Department of Physiology, Shantou University Medical College, Shantou, 515041, China
[c] Department of Pathology, Ganzhou Women and Children's Health Care Hospital, Ganzhou, 341000, China
[d] Department of General Surgery, The First Affiliated Hospital of Shantou University Medical College, Shantou, 515041, China
[e] Department of Pathology, Shantou University Medical College, Shantou, 515041, China

ARTICLE INFO

Keywords:
Breast cancer
miR-338–5p
Metastasis
ETS1
NOTCH1

ABSTRACT

Breast cancer ranks as the most prevalent cancer globally, surpassing lung cancer, with recurrence/metastasis to be its main account for the cancer-related mortality. MicroRNAs (miRNAs) participate critically in various physiological and pathological processes through post-transcriptional regulation of downstream genes. Our preliminary findings identified miR-338–5p, potentially linked to metastasis in breast cancer, a previously unexplored area. Analysis of the GSE38867 dataset revealed the decreased miR-338–5p expression in metastatic breast cancer compared to normal tissues. Cellular function experiments and a xenograft tumor model demonstrated the inhibitory function of miR-338–5p on the progression of breast cancer *in vitro* and *in vivo*. Furthermore, it downregulated the expression of mesenchymal biomarkers and NOTCH1 significantly. With the predicting targets of miR-338–5p and transcription factors of the NOTCH1 gene, coupled with dual luciferase reporter assays, it is identified ETS1 as the interactor between miR-338–5p and NOTCH1. In breast cancer tissues, as well as in our xenograft tumor model, expression of ETS1 and NOTCH1 was positively correlated using immunohistochemical staining. This study reports, for the first time, on the miR-338–5p/ETS1/NOTCH1 axis and its pivotal role in breast cancer proliferation and metastasis. These findings propose a novel therapeutic strategy for breast cancer patients and lays a foundation for its clinical detection and treatment evaluation.

1. Introduction

Breast cancer has emerged as the most prevalent malignancy among females, posing a significant global health threat. It is reported that, breast cancer, along with lung and colorectal cancers, collectively represent about 52 % of new female cancer cases, with breast cancer alone accounting for 31 %. The mortality rate of breast cancer ranks second highest among female cancer-related deaths [1].

* Corresponding author. The Breast Center, Cancer Hospital of Shantou University Medical College, Shantou, 515041, China.
E-mail address: jliu12@stu.edu.cn (J. Liu).
[1] These authors contributed equally.

https://doi.org/10.1016/j.heliyon.2024.e34949
Received 11 July 2024; Accepted 18 July 2024
Available online 20 July 2024

Although early diagnosis and the implementation of neoadjuvant chemotherapy and endocrine therapy have improved the treatment effectiveness and decreased the mortality rate of breast cancer patients, a substantial number still experience recurrence/metastasis, as the primary cause of cancer-related mortality in this population [2].

Among different molecular subtypes, triple-negative breast cancer (TNBC), well-known as the most aggressive one, exhibits the highest rates of recurrence/metastasis, along with the worst prognosis [3,4]. Because of lacking precise targets of treatment, TNBC therapeutics has become the key focus in the field of breast cancer research. The abnormal function of epithelial-mesenchymal transition (EMT) is considered as a prerequisite of the metastasis process from the primary location to distant sites [5]. External stimuli or gene changes lead to a decrease of adhesion complexes between epithelial cells and the destruction of the polarity of epithelial cells, causing corresponding changes in cytoskeletal proteins, thus transforming epithelial cells into mesenchymal cells. Interstitial cells have no polarity and lack the connection between adhesion complexes, so they can move in the extracellular matrix, which makes tumor cells have the potential to metastasize [6]. Important driving factors of EMT include Snail, ZEB1, EZH2, Twist, Slug and NOTCH1 [7–9]. TGF-β induces EMT by activating EMT-related transcription factors, including Snail1/2 and ZEB1/2 [10]. NOTCH signaling promotes EMT progress and angiogenesis of breast cancer tumor stem cells by activating the expression of ZEB1 [11]. Additionally, hypoxia can also induce NOTCH signaling, leading to induced EMT progress in breast cancer with decreased E-cadherin [12,13]. Given TNBC metastasis involves a complex, multi-step and multi-gene process, further research should focus on identifying effective diagnostic markers for various stages, particularly metastasis.

MiRNAs are a class of noncoding RNAs approximately 22 nucleotides in length, which bind to the 3′ untranslated region (3′UTR) of target mRNAs. They either cleave the target mRNA or inhibit translation through Ago2 ribonuclease in the RNA-induced silencing complex (RISC) [14]. The expression pattern of miRNA can be tissue-specific, and the imbalance of miRNA expression and its dysregulation of targeted genes contributes to the initiation and progression of cancer [15]. Previous investigation revealed that, miRNA expression shows significant imbalance detectable in breast cancer tissue samples, blood, serum, urine and/or other minimally invasive sources, indicating that miRNAs may have potential as prognostic and predictive biomarkers [16,17].

MiR-338 encompasses two mature sequences miR-338–3p and -5p, deriving from 3′ and 5′ sequences of the pre-miR-338 stem loop structure, respectively. The precursor of miR-338 is situated in the 8th intron of the AATK gene on chromosome 17 [18]. MiR-338 was first reported to be increased in membranes with chorioamnionitis associated with inflammation [19]. Soon, a role in controlling oligodendrocyte differentiation was found [20]. Our preliminary screening revealed low level of miR-338–5p in metastatic breast cancers compared to normal tissue. Meanwhile, in glioblastoma, miR-338–5p also acts predominantly as a tumor suppressor, inhibiting cellular proliferation and invasion [21,22], while in esophageal and gastric cancer, miR-338–5p influences tumor progression by targeting downstream genes, regarding the cisplatin resistance [23,24]. In addition, abnormal miR-338–5p expression was also observed in colorectal, lung, pancreatic and hepatocellular cancer [25–28]. However, its role in breast cancer remains unexplored, necessitating further investigation into the correlation between miR-338–5p and this disease. This study aims to elucidate the expression pattern and function role of miR-338–5p in breast cancer. Additionally, it seeks to characterize the molecular mechanisms involving miR-338–5p, providing experimental insights into the invasion and metastasis mechanisms of breast cancer, and provide potential treatment strategies and targets.

2. Materials and methods

2.1. The cell lines and culture

Human breast cancer cell lines, T47D, MCF-7, SKBR3, BT-549, and MDA-MB-231, along with normal human mammary epithelial cell HMEC, were obtained from ATCC, being cultured according to ATCC guidelines. Oligonucleotides of miRNA mimics/inhibitors and siRNA, and corresponding negative controls (Table 1) were purchased from GenePharma, Suzhou, China.

To examine the function and potential molecular mechanism, pLVX-miR-338–5p (pLVX-EGFP-IRES-puro as control vector), pGL3-NOTCH1-pro (the promoter region of NOTCH1 cloned in pGL3-enhancer) and pmir-ETS1-3′UTR (ETS1-3′UTR cloned in pmir-GLO) were purchased from Changsha Youbao Biotechnology (China). Mutant vectors were also created without the potential binding site.

Table 1
The sequences of the oligonucleotides.

Sequence	5′ → 3′
miR-338-5p mimic	AACAAUAUCCUGGUGCUGAGUG
	CUCAGCACCAGGAUAUUGUUUU
Mimic NC	UUCUCCGAACGUGUCACGUTT
	ACGUGACACGUUCGGAGAATT
miR-338-5p inhibitor	CACUCAGCACCAGGAUAUUGUU
Inhibitor NC	CAGUACUUUUGUGUAGUACAA
siETS1#1	ACUUGCUACCAUCCCGUAC
siETS1#2	GCAACACTTATGAAGATCCTCGAAT
siNC	UUCUCCGAACGUGUCACGUTT

2.2. RT-PCR

Total RNA was extracted using Trizol (Invitrogen, CA, USA), followed with synthesis of cDNA from mRNA and miRNA respectively. RT-PCR was conducted with specific primers (Table 2) using SYBR Select Master Mix on a Bio-Rad CFX96 Touch Real-time PCR Detection System.

2.3. Western blotting

Cells were lysed using RIPA lysis buffer supplemented with a protein phosphatase inhibitor and benzyl sulfonyl fluoride for 30 min. The collected supernatant was quantified regarding its protein concentration using a BCA assay kit (GenStar, China). Total protein was separated by SDS-polyacrylamide gel electrophoresis, transferred onto a PVDF membrane, and blocked by 5 % milk. The PVDF membrane with target proteins was then incubated at 4 °C overnight with primary antibodies (Table 3), followed by washing and incubation with corresponding secondary antibodies at room temperature for 2 h. Target proteins were visualized and detected using enhanced chemiluminescence reagents (Thermo Fisher, USA) under the chemiluminescent imaging system (Bio-Rad ChemiDoc XRS+, USA).

2.4. Cell Counting Kit-8 assay and colony formation

Pretreated cells were resuspended and inoculated into 96-well plates. Cell viability was assessed using the Cell Counting Kit-8 (CCK8) reagent at a continuous timepoint after seeding. Following a 2-h incubation with CCK8 reagent, absorbance was measured at 450 nm using a SpectraMax M5 (California, USA).

Pretreated cells were resuspended and inoculated into six-well plates for continuous culture. Once macroscopic cell colonies appeared, crystal violet staining was performed, and formed colonies were counted and quantified using a Zeiss microscope.

2.5. Wound healing assay

Upon reaching confluence in six-well plates, cells were subjected to a 2 mm-wide scratching wound using 200-μl tips. Subsequently, continuous culture was conducted with photographing the wound width at specific timepoints after scratching. Wound closure was assessed and measured under a Zeiss microscope by the width of the injury line.

2.6. Transwell assay

To evaluate the migratory/invasive ability of cells, the transwell assay was conducted with or without Matrigel. Pretreated cells were resuspended in DMEM without FBS and inoculated into upper chamber, and full DMEM was added into lower chamber. Cells were allowed to migrate for 24 h and invade for 36 h in a humidified atmosphere with 5 % CO_2 at 37 °C. Those on the lower side of upper chamber were stained with crystal violet and calculated under a Zeiss microscope by two independent researchers.

2.7. Cellular apoptosis

Pretreated cells were resuspended in a binding buffer supplemented with 5 μL of Annexin V-FITC (C1063, Beyotime, China). Following a 20-min incubation at room temperature, 10 μL of PI was added and further incubated for 10 min. The apoptotic cells were assessed using Accuri C6 Flow Cytometry (Becton-Dickinson, USA).

2.8. Immunofluorescence

Pretreated cells were collected and inoculated into a Millicell EZ Slide (Merck Millipore). After adhering to the slide, the cells were fixed with 4 % paraformaldehyde at room temperature. Subsequently, the cells were permeabilized with Triton X-100, following by

Table 2
The sequences of specific primers for RT-PCR.

Primers	5' → 3′
β-Actin	F: GCTGATGCTGAAGTGTGGTG
	R: AGCGAGCATCCCCAAAGTT
NOTCH1	F: CGGGTCCACCAGTTTGAATG
	R: GTTGTATTGGTTCGGCACCAT
ETS1	F: CCCGTACGTCCCCCACTCCT
	R: TGGGACATCTGCACATTCCA
U6	F: AACGCTTCACGAATTTGCGT
	R: CTCGCTTCGGCAGCACA
miR-338–5p	F: AACAATATCCTGGTGCTGAGT
	R: AGTGCAGGGTCCGAGGTATT

Table 3
Antibody information.

Antibody	kDa	Source	Company	Cat#
β-Actin	42	Mouse IgG	CST	3700 S
ETS1	50	Rabbit IgG	CST	14069 S
GAPDH	37	Mouse IgG	ZSGB-BIO	16AF0412
NOTCH1	120	Rabbit IgG	CST	3439 S
Vimentin	57	Rabbit IgG	CST	5741 S
EZH2	98	Rabbit IgG	CST	5246 T
Bcl-2	26	Rabbit IgG	CST	4223 S
Caspase-3	30	Rabbit IgG	CST	9662 S
Cleaved caspase-3	17	Rabbit IgG	CST	9661 S

blocking using 5 % BSA at room temperature. For F-actin and α-tubulin, the glass slide was incubated with F-actin antibody (Invitrogen, 2157163) and anti-α-tubulin (Invitrogen, 2273689) for 30 min at room temperature, while for ETS1 (CST, 14069 S) and NOTCH1 (CST, 4380 S), primary antibodies were diluted at ratio of 1:200 in PBS and incubated on the slide at 4 °C overnight. Then, after washing, the slides were incubated with corresponding fluorescent secondary antibodies (CST, 8889 S or 4408 S) at room temperature. Then, the nucleus was stained with DAPI for 5 min. Finally, slides were mounted and photographed.

2.9. Dual-luciferase reporter assay

To verify the regulatory mechanism of miR-338–5p/ETS1 axis, cells were co-transfected with pRL-SV40 and reporter vector, along with varying concentrations of the miR-338–5p mimic. For exploring the transcriptional regulation of ETS1 on NOTCH1 expression, cells were co-transfected with pRL-SV40 and reporter vector, along with varying concentrations of pCDNA3.1-ETS1-HA. Luciferase activities with different substrates were assessed using the Dual-Luciferase Reporter Assay Kit (E1910, Promega).

2.10. Chromatin immunoprecipitation (ChIP) assay

A ChIP assay kit (Beyotime, P2078) was employed to evaluate the binding potential between ETS1 and NOTCH1 promoter region, following the manufacturer's instructions. Initially, the fixed cells by formaldehyde were ultrasonicated. Samples were then pre-washed with protein A + G beads for 1 h, followed by an overnight incubation with either anti-ETS1 antibody or IgG as negative control. After washing and eluting the beads, the cross-linking was reversed, and protein was digested with protease K. A DNA purification kit (Beyotime, D0033) was applied to purify DNA for further PCR amplification. Sequences of primers used in ChIP assays were as follows: CSL binding site-F: CAGGGACTATGGCAGGCATT; CSL binding site-R: CCTAAGGTGGCCCCAGAAAG; negative control-F: CAGCTGTCCATGGGGTACTC; negative control-R: CAGCAGAGAAGAGAGTGGCC.

2.11. Xenograft tumor model

8 Nu/Nu mice were randomly allocated into two groups and injected subcutaneously with MDA-MB-231 cells overexpressing miR-338–5p or negative control cells. Two weeks after injection, tumor volume was evaluated every three days, calculated using the following formula, volume = length × width^2 × 1/2. Finally, tumors were excised and fixed in paraformaldehyde for further immunohistochemical staining. The animal experiments were conducted with approval from the Animal Ethics Committee of Shantou University Medical College (SUMC-2021-203), in compliance with relevant ethical regulations governing animal research.

2.12. Immunohistochemical staining

Standard procedures were conducted on 4 μm-thick slices with dewaxing, rehydration, epitope recovery, and inactivation of endogenous peroxidase activity. Sections were incubated with primary antibodies at 4 °C overnight or PBS as negative control, followed by visualization using 3,3′-diaminobenzidine tetrahydrochloride. Evaluation was independently conducted by two researchers using a bright field microscope. Staining intensity was divided into four grades: 0–3. The percentage of positive cells was scored as follows: 0 indicating 0 %, 1 for 1%–25 %, 2 represented 26%–50 %, 3 presenting 51%–75 %, and 4 as 76%–100 %. Finally, the total expression score, comprising staining intensity and percentage of positive cells, was categorized into two groups: low (score $\leq$3) and high (score $\geq$4). Ethical approval was obtained from the Ethics Committee of Shantou University Medical College (SUMC-2021-50), and all procedures adhered to the guidelines outlined in the Declaration of Helsinki.

2.13. Bioinformatics analyses

Differentially-expressed miRNAs between metastatic breast cancer tissues and adjacent tissues were identified using dataset GSE38867 [29]. Additionally, the GSE40525 [30], CancerMIRNome [31] and ENCORI [32] databases were also used to evaluate the expression pattern of miR-338–5p accordingly. The expression profiles of miR-338–5p in TNBC tissues versus non-TNBC tissues were sourced from the GSE58606 [33]. The prognostic significance of miR-338–5p in breast cancer patients was evaluated using the

OncoLnc database (http://www.oncolnc.org/).

Potential target genes of miR-338–5p were assessed by miRDB [34] and DIANA [35] and intersected by Venn diagraming. Using the hTFtarget database [36] to predict potential transcription factors of NOTCH1, sequences of the ETS1 3′UTR and NOTCH1 promoter were searched and downloaded from NCBI (https://www.ncbi.nlm.nih.gov/). The JASPAR database was employed to predict the potential binding location of ETS1 on the NOTCH1 promoter [37].

Correlation of the expressions of miR-338–5p, ETS1 and NOTCH1 was analyzed using the cBioPortal database (TCGA, Nature 2012) [38]. To assess the prognostic significance of ETS1 and NOTCH1, Kaplan-Meier analysis was conducted using publicly available datasets. Specifically, GSE1992 [39] was utilized for overall survival (OS) and recurrence-free survival (RFS), GSE10886 [40] for RFS, and GSE37181 [41] for distant metastasis-free survival (DMFS) through the PanCanSurvPlot tool (https://smuonco.shinyapps.io/PanCanSurvPlot/).

2.14. Statistical analysis

Each experiment in this study was replicated at least three times. Student's t-test and one-way ANOVA were used for continuous variables, while categorical variables were assessed using the chi-square test or Fisher's exact test. The relationship was evaluated by the Spearman rank correlation test. The $p < 0.05$ was considered with statistical significance.

3. Results

3.1. The miR-338–5p level is suppressed in breast cancer and associated with poor prognosis

To explore potential miRNAs related to metastasis, the GSE38867 dataset was recruited to analyze differential-expressed miRNAs in metastatic breast cancer compared to adjacents. Using a significance cutoff of $p < 0.05$, along with $|\log FC| > 2$, the top 20 down-

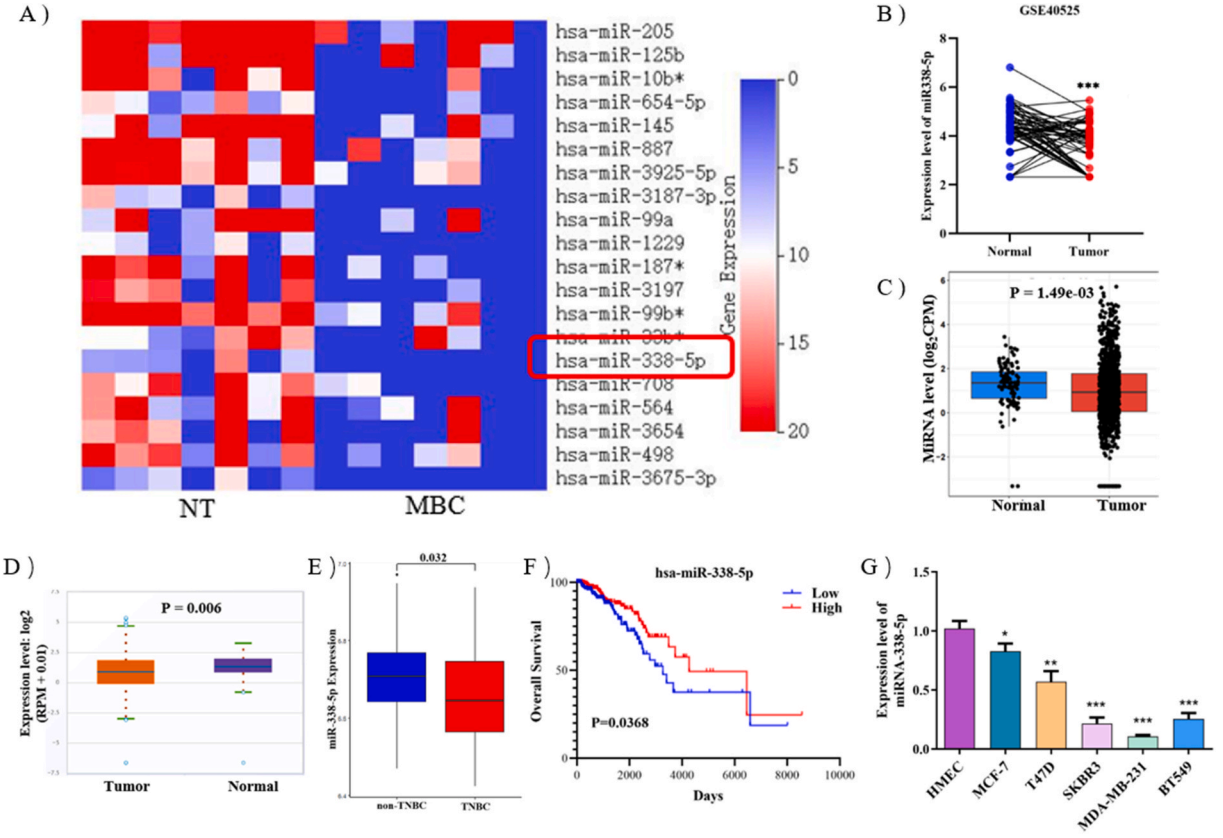

Fig. 1. The miR-338-5p level is low in metastatic breast cancers. (A) Top 20 downregulated miRNAs in metastatic breast cancers (MBC) compared to normal tissues (NT), based on analysis of the GSE38867 dataset. (B) Low miR-338–5p expression observed in breast cancer tumors in GSE40525 ($p < 0.05$). (C) The miR-338–5p level analyzed on the CancerMIRNome database ($p = 1.49e\text{-}03$). (D) The low miR-338–5p level revealed by ENCORI database ($p = 0.006$). (E) The low miR-338–5p expression in TNBC (N = 31) compared to non-TNBC (N = 91), analyzed with GSE58606 database ($p < 0.05$). (F) Low miR-338–5p expression correlated with poor overall survival among patients with breast cancer ($p = 0.0368$). (G) High level of MiR-338–5p in normal mammary epithelial cells, while low in breast cancer cell lines, especially in TNBC cell lines.

regulated miRNAs are shown in Fig. 1A. Among them, miR-338–5p had not been previously reported in breast cancer. To validate its expression pattern, additional datasets were applied, confirming a decreased level of miR-338–5p in breast cancer tissues (Fig. 1B-D). Moreover, miR-338–5p expression was significantly low in TNBC tissues compared to non-TNBC tissues (Fig. 1E).

To predict the potential impact of reduced miR-338–5p expression in breast cancers, OS was analyzed based on miR-338–5p levels, indicating that low miR-338–5p levels were associated with poor prognosis (Fig. 1F). Furthermore, examination of miR-338–5p expression across various breast cancer cells and normal HMEC cells revealed decreased level of miR-338–5p in breast cancer cell lines compared to normal counterparts, particularly in TNBC cell lines, MDA-MB-231 and BT-549 (Fig. 1G).

3.2. Overexpressing miR-338–5p suppresses cellular proliferation and increases apoptotic cells in TNBC

Overexpressing miR-338–5p with a mimic was successfully achieved in TNBC cells, MDA-MB-231 and BT549 (Fig. 2A-B). CCK-8 and colony formation assays demonstrated that miR-338–5p overexpression suppressed cellular proliferation and the formation of colonies in breast cancer cells (Fig. 2C-E). Furthermore, elevated miR-338–5p expression induced apoptosis in these cells, increasing the proportion of early apoptosis from 8.1 % to 5.3 %–15 % and 19.7 %, respectively (Fig. 2G-H). To confirm the enhanced apoptosis, biomarkers of apoptosis were examined. Consistently, the level of activated and cleaved caspase-3 was increased accordingly, while Bcl-2, the anti-apoptotic protein was suppressed by miR-338–5p (Fig. 2F).

3.3. Motility of TNBC cells is inhibited with overexpressing miR-338–5p

To evaluate the impact of miR-338–5p on breast cancer cell motility, wound healing assays and transwell experiments were conducted. Overexpression of miR-338–5p notably prevented the wound closure in TNBC cells during the continuous culture after scratching (Fig. 3A and B). Similarly, transwell migration and invasion were also suppressed by overexpressing miR-338–5p in both cell lines (Fig. 3C and D). Expression of mesenchymal phenotypic biomarkers, EZH2, vimentin and ZEB1, as well as the NOTCH1 oncogene, were decreased in cells overexpressing miR-338–5p (Fig. 3E), which has been found to be associated with EMT [8,12,13].

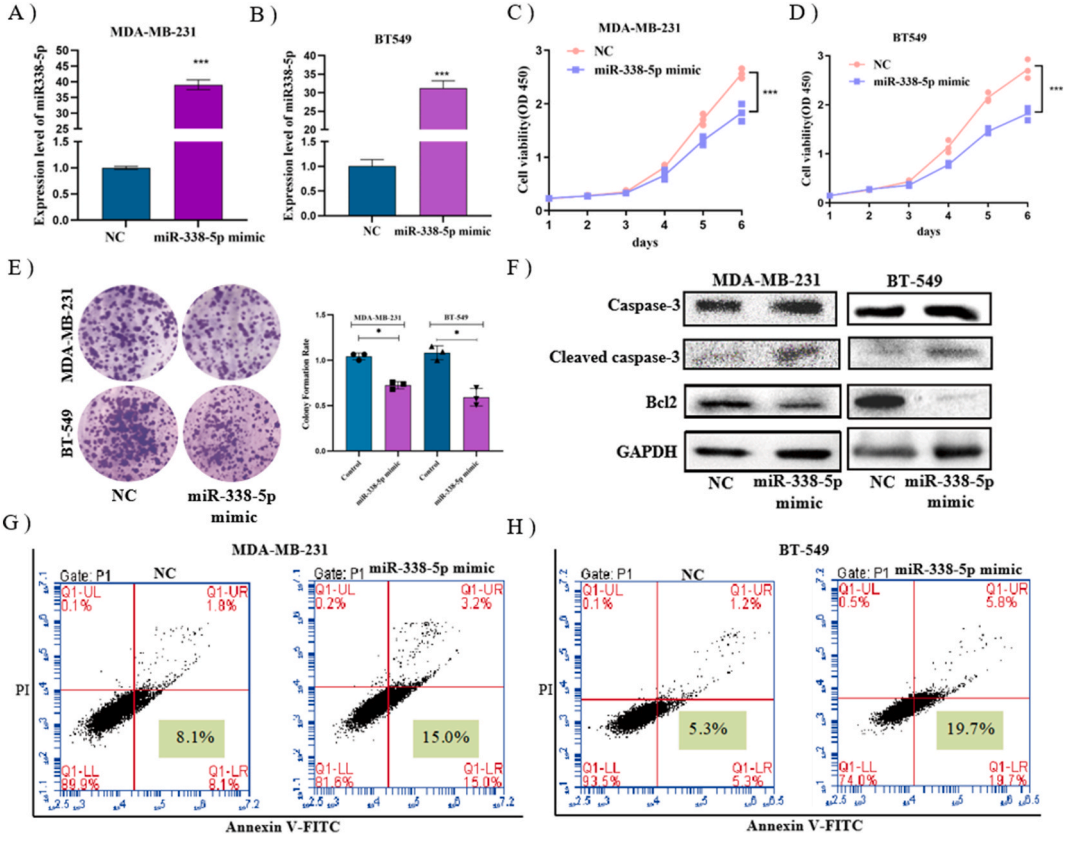

Fig. 2. Overexpressing miR-338-5p suppresses cellular proliferation and increases apoptotic cells of TNBC. (A–B) RT-PCR confirming the successfully increased miR-338–5p expression in TNBC cells transfecting miR-338–5p mimic. (C–D) The inhibited cellular proliferation by overexpressing miR-338–5p. (E) The decreased colonies formed by MDA-MB-231 and BT-549 cells with high miR-338–5p level. (F) With overexpressed miR-338–5p, upregulated apoptosis-inducing markers (cleaved caspase-3) and downregulated anti-apoptosis markers (Bcl-2) in TNBC cells. (G–H) The increased apoptotic cells by miR-338–5p overexpression.

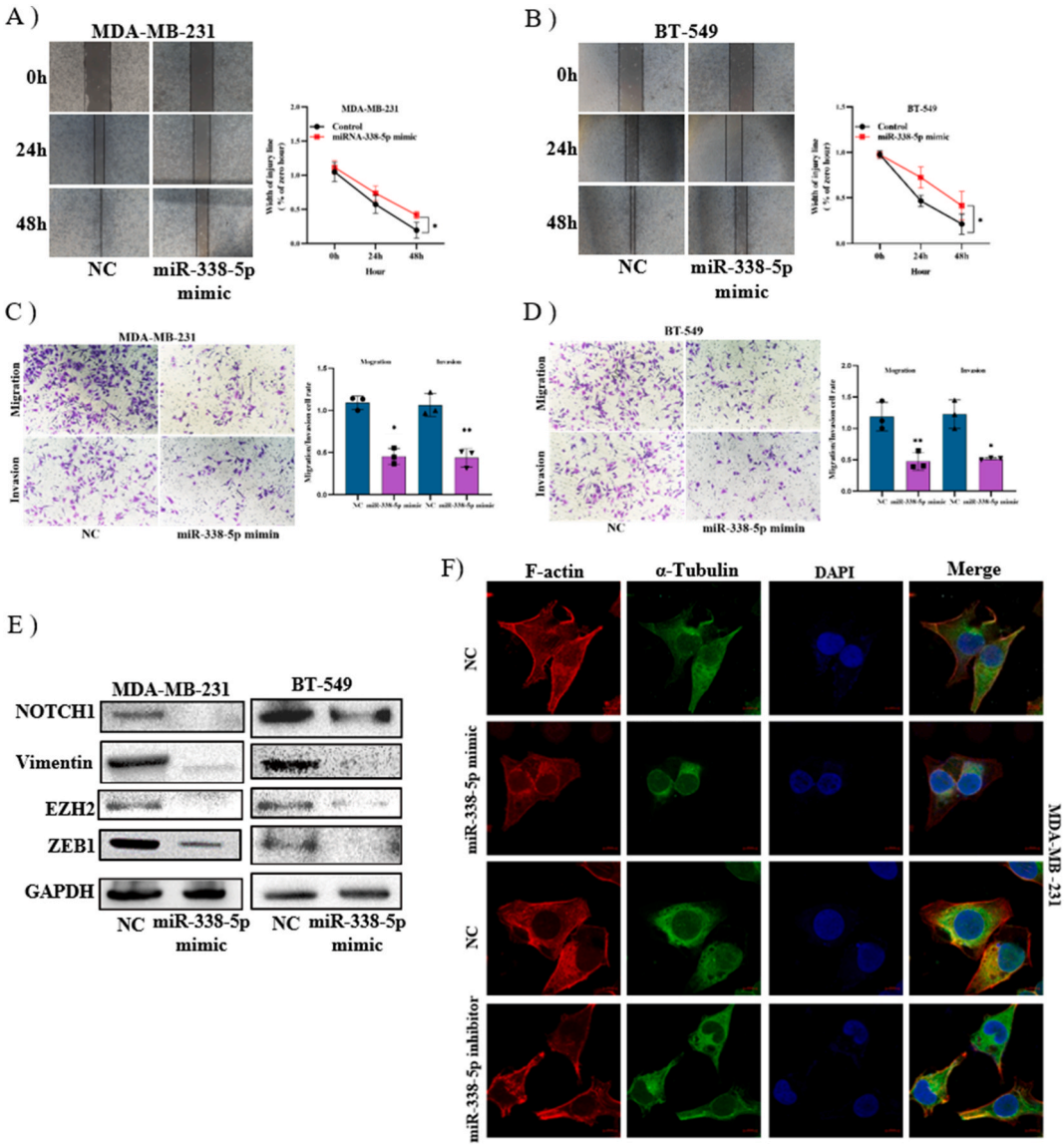

Fig. 3. Motility of TNBC cells is inhibited by overexpressed miR-338-5p. (A–B) After overexpressing miR-338–5p mimic, the wound healing abilities of TNBC cells were reduced. (C–D) Overexpressed miR-338–5p suppressed migratory/invasive abilities of TNBC cells. (E) Increased miR-338–5p decreased the level of mesenchymal markers in TNBC cells. (F) Overexpressed miR-338–5p inhibited formation of cellular cytoskeleton (F-actin and α-tubulin) in TNBC cells (magnification 630 ×).

Motility of cells is associated with their cytoskeleton components. Immunofluorescence staining revealed that with overexpressed miR-338–5p, the filamentous arrangement of F-actin was suppressed and eliminated in those cells, the formation of dense foci increased, and the pseudopod-like peripheral processes around cells decreased. The fluorescence intensity of α-tubulin in cells was also reduced. Conversely, silencing miR-338–5p produced opposite effects (Fig. 3F), suggesting a role for miR-338–5p in maintaining the cytoskeletal structure of breast cancer cells, thereby suppressing their migratory/invasive abilities.

3.4. MiR-338–5p represents its tumor suppressor role by suppressing ETS1 translation

To further elucidate how miR-338–5p inhibits breast cancer, miRDB and DIANA databases were analyzed to identify potential downstream targets of miR-338–5p (Fig. 4A). When determining the miR-338–5p effect on EMT, NOTCH1 was detected to be also decreased in overexpressed miR-338–5p cells, along with mesenchymal biomarkers (Fig. 3E), suggesting that miR-338–5p may represent its function by suppressing the NOTCH1 signaling pathway. NOTCH1 is well-known to promote the metastasis of breast cancer, and our research group has been engaged in the research on the NOTCH family members in breast cancer development [42]. Previous studies revealed that NOTCH1 activated AKT pathway and promoted EMT of breast cancer partly by directly activating MVP

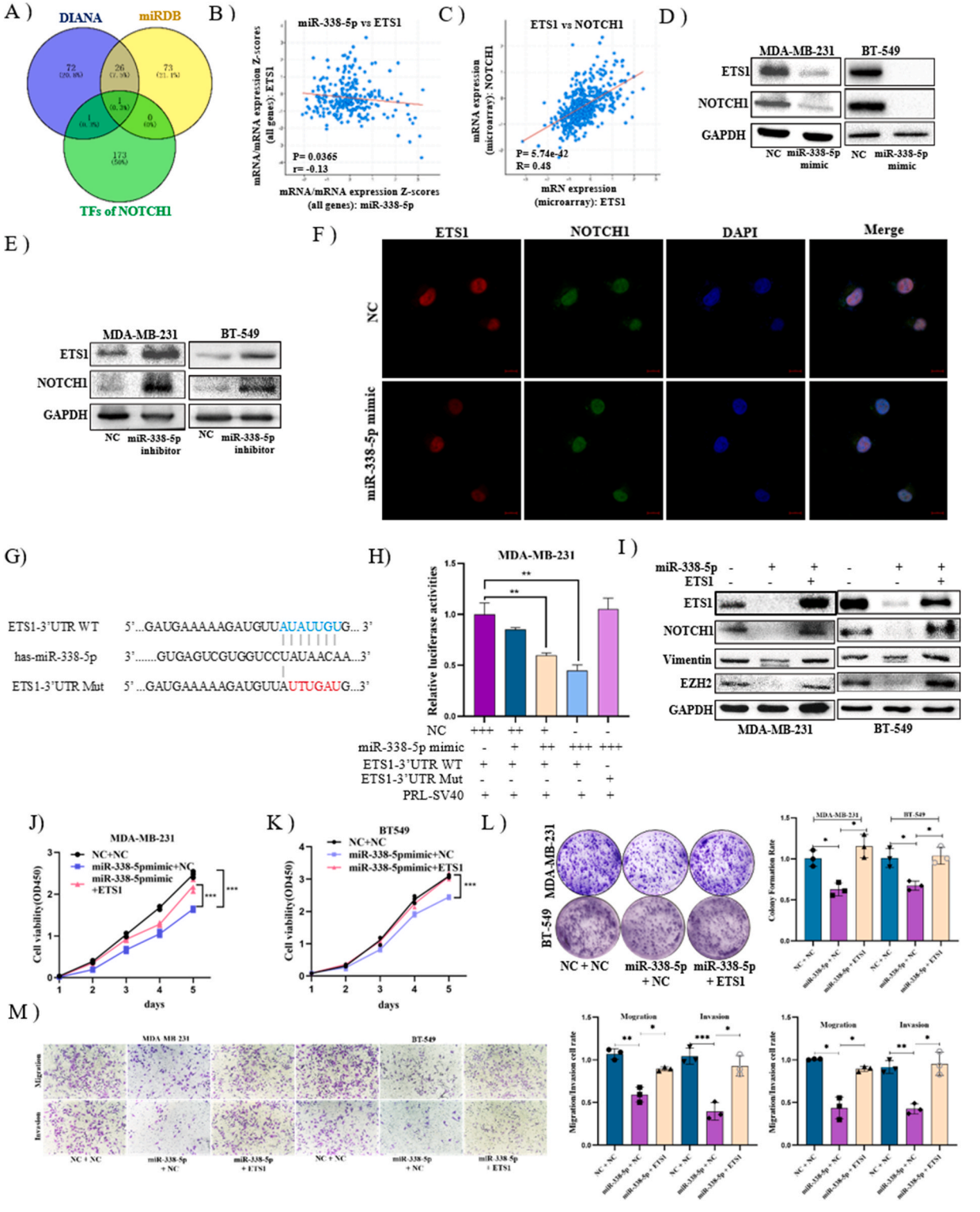

(caption on next page)

Fig. 4. MiR-338-5p represents its anti-cancer function through inhibiting ETS1. (A) ETS1, the commonly predicted miR-338–5p target genes and potential transcription factors regulating NOTCH1. (B–C) Relationship between miR-338–5p/ETS1 or ETS1/NOTCH1 in breast cancer tissues. (D–E) Increasing miR-338–5p decreased both ETS1 and NOTCH1 level in TNBC cells, and vice versa. (F) Fluorescence intensity of ETS1 and NOTCH1 staining was suppressed by a miR-338–5p in MDA-MB-231 cells (magnification 400 ×). (G) Predicted core site for miR-338–5p, along with its binding sequences in ETS1-3′UTR. (H) In MDA-MB-231 cells, miR-338–5p inhibited luciferase activities of the ETS1-3′UTR reporter, but not the mutant reporter, in a dose-dependent manner. (I) Transfection of miR-338–5p into TNBC cells decreased ETS1 expression and mesenchymal markers, while co-transfection of miR-338–5p and ETS1 restored their expression accordingly. (J–L) Rescue experiments with CCK-8 and colony formation demonstrated that ETS1 can reverse the inhibitory effect of miR-338–5p on cell proliferation. (M) Rescue experiments as transwell assay revealed that ETS1 can reverse the inhibitory effect of miR-338–5p on cell migration/invasion.

[43]. In addition, NOTCH1 was investigated to combine with CD73 promoter region directly and increase its transcription activities accordingly, which provides a new mechanism for TNBC cisplatin resistance mechanism [44]. However, no binding site was not predicted in 3′UTR of NOTCH1 for miR-338–5p. After screening for potential transcriptional factors regulating NOTCH1, ETS proto-oncogene 1 (ETS1) mRNA was emerged as potential target of miR-338–5p (Fig. 4A).

In Fig. 4B-C, it illustrated the correlations among miR-338–5p, ETS1, and NOTCH1 expressions in breast cancer patients, confirming the prediction of miR-338–5p/ETS1/NOTCH1 axis. Specifically, miR-338–5p exhibited a negative correlation with ETS1 mRNA, whereas ETS1 mRNA showed a positive correlation with NOTCH1 mRNA. As expected, the expression of ETS1 was decreased in overexpressed miR-338–5p cells, in parallel with the decreased NOTCH1 levels in TNBC cells (Fig. 4D). Conversely, treatment with miR-338–5p inhibitor yielded opposite effects (Fig. 4E). Immunofluorescence staining further demonstrated reduced fluorescence intensity of both ETS1 and NOTCH1 following miR-338–5p overexpression in MDA-MB-231 cells (Fig. 4F).

The potential core miR-338–5p binding location in ETS1-3′UTR region is displayed in Fig. 4G, and was used to construct the reporter vector, pmir-ETS1-3′UTR, as well as a mutant ETS1-3′UTR containing a mutated miR-338-5-p binding site. In dual-luciferase reporter assays, the luciferase activities regulated by ETS1-3′UTR were dose-dependently suppressed by miR-338–5p, whereas no change was observed in mutant group (Fig. 4H). To investigate whether miR-338–5p represents its anti-cancer effects through suppressing ETS1, rescue experiments were designed to re-express ETS1 in overexpressed-miR-338–5p TNBC cells. Expression of mesenchymal biomarkers, vimentin and EZH2, were decreased in cells with high miR-338–5p but was restored by re-expressing ETS1. Additionally, NOTCH1, decreased by miR-338–5p overexpression, was also upregulated by re-expressing ETS1 (Fig. 4I).

In cellular function experiments, the suppression of proliferation by miR-338–5p was reversed by re-expressing EST1 (Fig. 4J–K). Similarly, the number and size of colonies formed decreased with increased miR-338–5p level, but were restored by re-expressing ETS1 (Fig. 4L). Furthermore, in transwell assays, the migratory/invasive abilities of breast cancer cells were also restored by ETS1 re-expression in the presence of miR-338–5p overexpression (Fig. 4M). These findings suggest that miR-338–5p represents its tumor suppressor function through inhibiting ETS1 expression, at least partly.

3.5. The biological function of ETS1 can be attenuated by suppressing NOTCH1, its direct downstream gene

NOTCH1 was down-regulated by knockdown of ETS1 expression in TNBC cells, both at mRNA and protein levels (Fig. 5A–C). ChIP and dual-luciferase assays were conducted to validate ETS1's regulatory role on NOTCH1 in breast cancer. Using the JASPAR database, the classic binding motif of ETS1 was predicted on promoter region of NOTCH1 (Fig. 5D), identifying two potential ETS1 binding sequences in the NOTCH1 promoter region, namely −940 ~ −936 and −927 ~ −922. Because of the proximity of these two binding sites, only one pair of ChIP primers was designed for amplifying the NOTCH1 promoter containing two potential binding sequences (Fig. 5E). ChIP results indicated direct binding of ETS1 to the NOTCH1 promoter region (Fig. 5F). Furthermore, luciferase assays demonstrated that ETS1 enhanced luciferase activities driven by the wild-type NOTCH1 promoter in a concentration-dependent manner, whereas the activities driven by mutant NOTCH1 promoter remained unaffected by ETS1 expression levels (Fig. 5G). These findings established that ETS1 binds to NOTCH1 promoter directly, thereby modulating its transcriptional activity and augmenting NOTCH1 expression.

The rescue experiments were designed to validate ETS1/NOTCH1 axis role in breast cancer. While siETS1 suppressed NOTCH1 expression, re-expression of NOTCH1, in siETS1 treated cells, increased NOTCH1 levels both in mRNA and protein (Fig. 5H–J) and restored cellular proliferation, and migratory/invasive abilities, which were initially inhibited by ETS1 silencing (Fig. 5K–N). This indicates that ETS1, targeted by miR-338–5p, functions its oncogenic role in breast cancer through transcriptionally activating NOTCH1.

3.6. In vivo, miR-338–5p inhibits breast cancer progression through the ETS1/NOTCH1 axis

To assess the impact of miR-338–5p *in vivo*, we established a subcutaneous xenograft tumor model in Nu/Nu mice. In Fig. 6A and B, tumors overexpressing miR-338–5p exhibited significantly smaller volumes compared to the control group. At the experimental endpoint, the removed tumors were stained to detect the downstream associated biomarkers. Notably, miR-338–5p overexpression correlated with reduced levels of ETS1 and NOTCH1 in the *ex vivo* tumor tissues. In addition, the Ki-67 index and vimentin expression in miR-338–5p overexpression tumor tissue were also decreased accordingly (Fig. 6C), indicating that increased miR-338–5p suppressed the tumor growth *in vivo*, along with reduced the level of mesenchymal biomarkers.

To verify this relationship at the clinical level, the expression of ETS1 and NOTCH1 was investigated among 135 cases of breast cancer. Immunohistochemical staining showed that ETS1 was mainly expressed in nucleus, while NOTCH1 was in both nucleus and

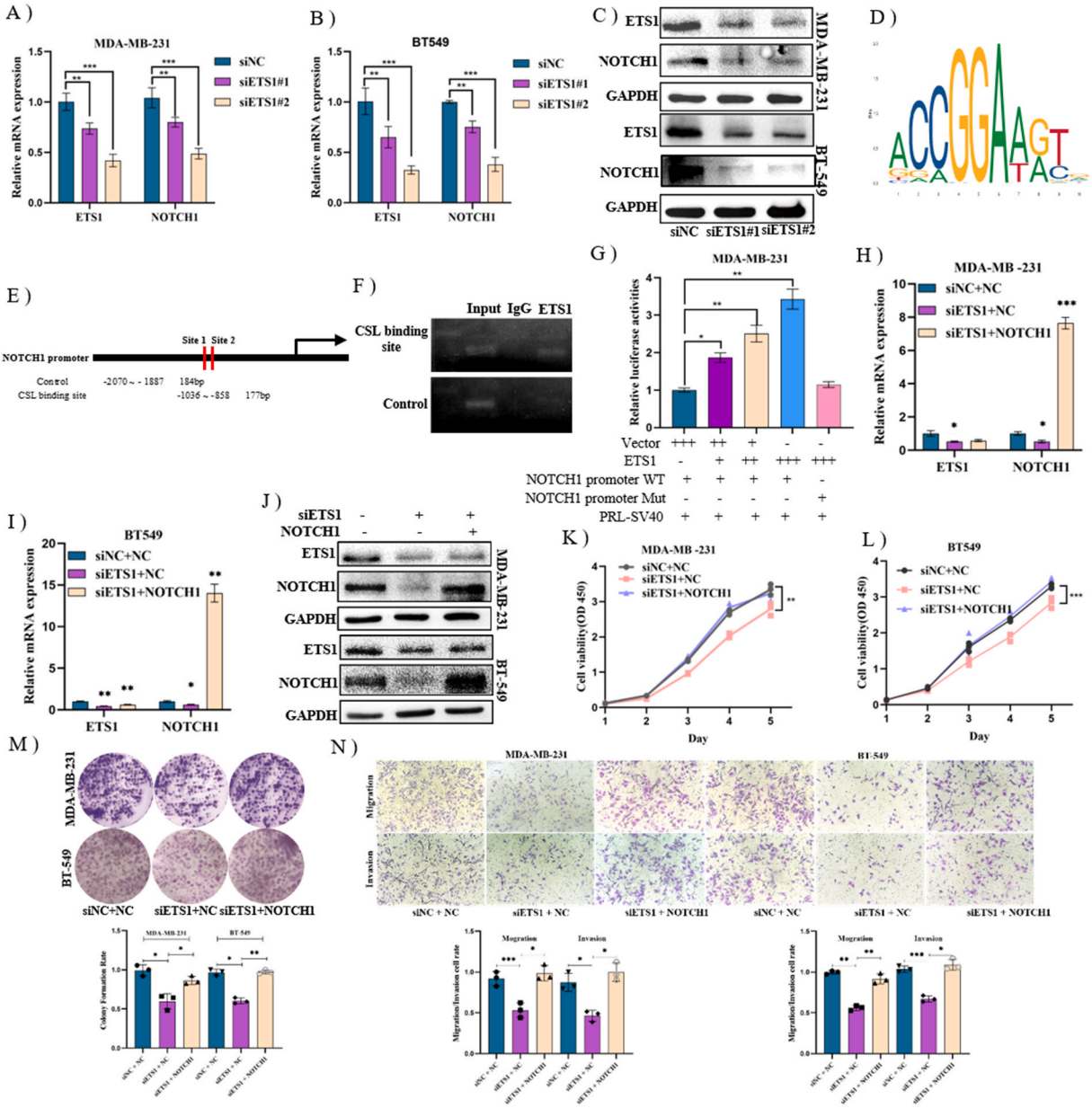

Fig. 5. Biological function of siETS1 can be attenuated by its direct downstream target, NOTCH1. (A–C) RT-PCR and western blotting showing that after transfecting siETS1 into TNBC cells, the expression of NOTCH1 decreased. (D) JASPAR database-predicted ETS1-binding motif in the NOTCH1 promoter region. (E) The NOTCH1 promoter region with ETS1 binding potential, and the strategy for ChIP primer design. (F) ChIP showed that ETS1 antibody could precipitate the corresponding DNA fragment in the NOTCH1 promoter. (G) In MDA-MB-231 cells, luciferase activities driven by the NOTCH1 promoter increased with increased ETS1 levels but remained unchanged with the mutant plasmid. (H–J) Knockdown of ETS1 using siETS1 in TNBC cells decreased NOTCH1 expression compared to controls, which was restored upon co-transfection with siETS1 and NOTCH1. (K–M) CCK-8 and colony formation assays showed that the effect of siETS1 on cell proliferation can be restored by re-expressing NOTCH1. (N) Transwell assay indicating that the efforts of siETS1 on cellular migratory/invasive abilities can be restored by re-expressing NOTCH1.

cytoplasm/membrane (Fig. 7A). Statistics show that in 135 cases of breast cancer tissues, 70.37 % showed high expression of ETS1, and 89.63 % showed high expression of NOTCH1. In breast cancer tissues, both ETS1 and NOTCH1 are highly expressed ($p = 0.000$, Table 4). We also analyzed the staining intensity of ETS1 and NOTCH1 according to different degrees of staining, revealing a positive correlation between the expression levels of ETS1 and NOTCH1 ($p = 0.021$ and $r = 0.199$, Table 5).

To assess the prognostic significance of ETS1/NOTCH1 axis among breast cancer patients, we categorized patients into low or high expression groups using the optimal (maximum choice grade statistics) method in the PanCanSurvPlot database. We evaluated the

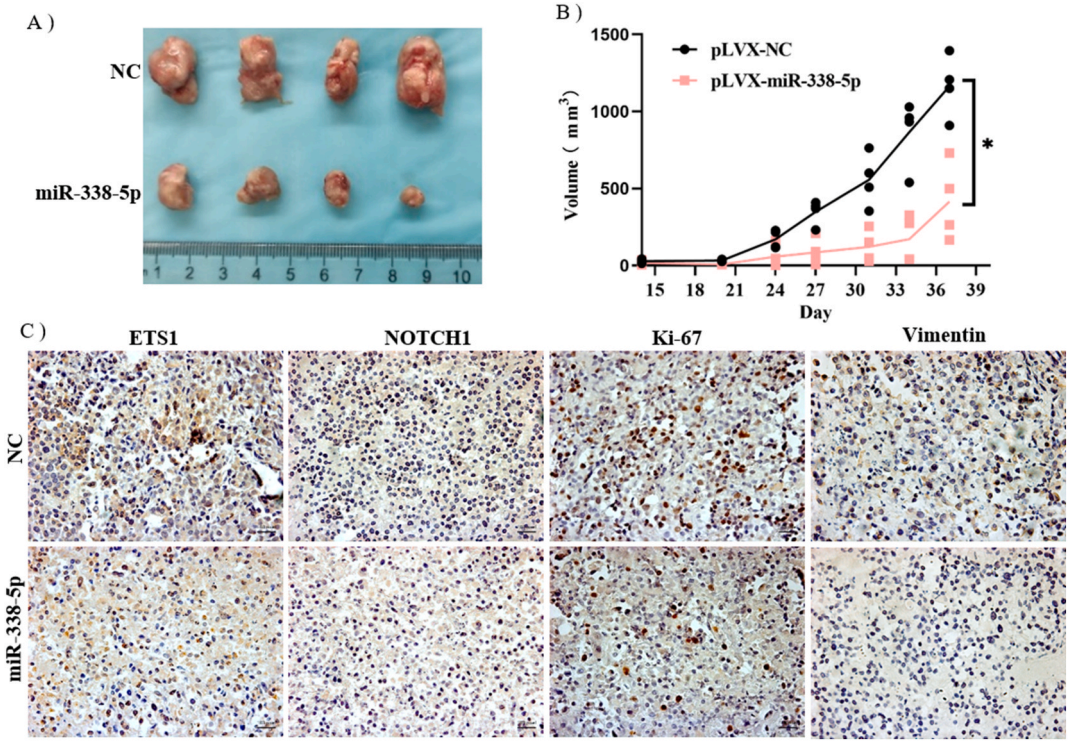

Fig. 6. MiR-338-5p inhibits breast cancer progression *in vivo* through the ETS1/NOTCH1 axis. (A) The volume of subcutaneous tumors in mice overexpressing miR-338–5p was significantly reduced compared to the control group. (B) Growth curves of subcutaneous xenograft tumors in mice showing that miR-338–5p overexpression inhibited tumor growth. (C) *Ex vivo*, the level of ETS1, NOTCH1, Ki-67 and mesenchymal markers was decreased (magnification 200 ×).

prognostic value of ETS1 and NOTCH1 in terms of OS, RFS, and DMFS. It is indicated that reduced levels of ETS1 or NOTCH1 were correlated with increased OS among breast cancer patients (Fig. 7B/7 F). Additionally, their potential in predicting breast cancer recurrence was assessed, revealing that patients with low ETS1 or NOTCH1 expression frequently exhibited prolonged RFS (Fig. 7C/7D/7G/7H). Given that metastasis significantly impacts patient prognosis in malignancies, we also evaluated the prognostic role of ETS1 and NOTCH1 in predicting breast cancer metastasis. Lower expression levels of ETS1 or NOTCH1 were associated with extended DMFS in breast cancer patients (Fig. 7E/7I).

4. Discussion

By screening for potential biomarker miRNAs in breast cancer patients, this study reports the tumor inhibitory effect of miR-338–5p in breast cancer, revealing a new miR-338–5p/ETS1/NOTCH1 axis responsible for inhibiting the proliferation and invasion of breast cancers. The emerging role of non-coding miRNAs in tumorigenesis, particularly in breast cancer, is gradually being elucidated. It has been identified miRNAs as significant contributors to tumor metastasis. For instance, miR-221 has been highlighted as a crucial factor in inducing EMT process [45], while miR-140–5p performs anti-cancer roles through reducing the formation of capillaries and inhibiting the growth of tumors [46]. Nevertheless, the role and molecular regulation of miRNAs in breast cancer at this stage is only the tip of the iceberg, and needs further exploration and research.

We conducted a differential expression analysis of miRNAs in metastatic breast cancer compared to matched normal tissues, identifying miR-338–5p as playing a significant role in breast cancer metastasis. Previous research has highlighted miR-338–5p′s tumor suppressor role across various malignancies, including lung, gastric, prostate, esophageal cancers, and glioma [22,23,26,47,48], consistent with our findings in breast cancer. Our study revealed down-regulation of miR-338–5p in breast cancer tissues and cells, correlating high miR-338–5p expression with favorable prognosis in breast cancer patients. Overexpressing miR-338–5p can inhibit breast cancer cell proliferation, colony formation, wound healing, migration/invasion, and induce apoptosis, whereas knocking down miR-338–5p produces opposite efforts. Animal experiments confirmed miR-338–5p′s inhibitory effect on breast cancer *in vivo*. However, increased miR-338–5p level has been reported in colorectal cancer, liver cancer, melanoma and retinoblastoma, and may be related to the tissue specificity of miR-338–5p expression and the microenvironment of different tumors [25,28,49,50]. Although some studies have reported a carcinogenic role of miR-338–5p in tumors, most reports are consistent with our results in breast cancer, that is, miR-338–5p represents the inhibitory function in most malignancies, including breast cancer.

MiR-338–5p, a non-coding small RNA, exerts significant influence on tumor initiation and progression by targeting various

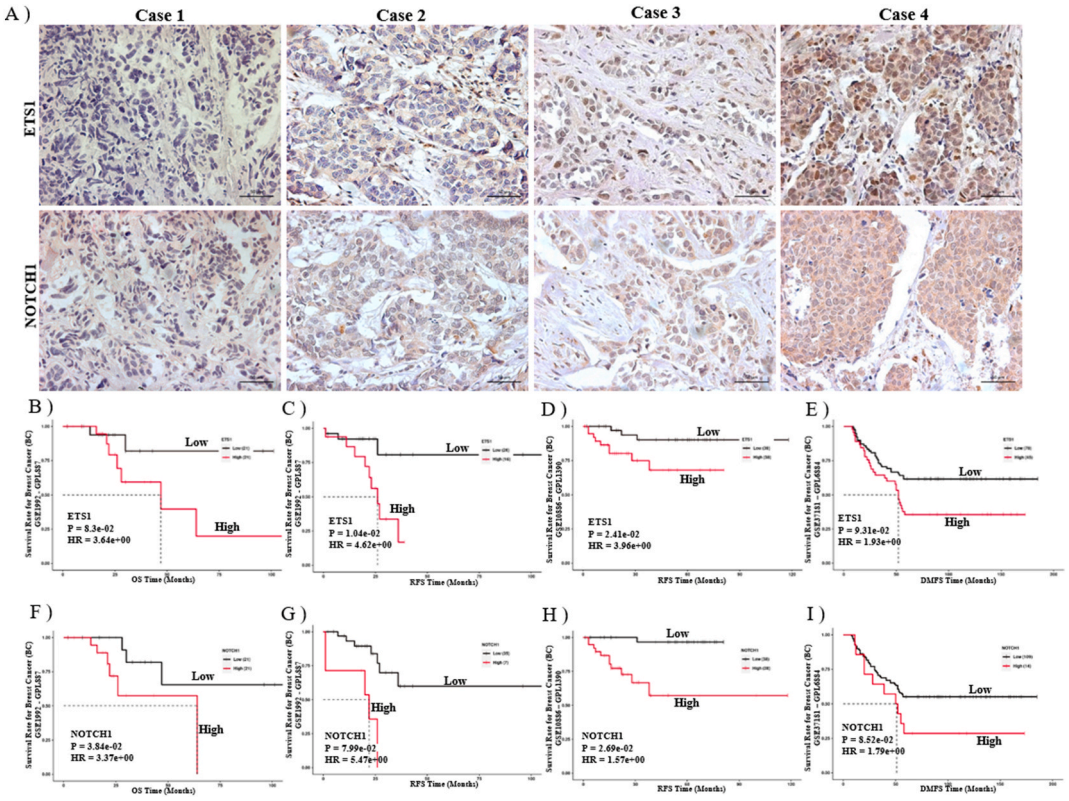

Fig. 7. Expression and prognosis based on ETS1 andNOTCH**1 in clinical breast cancer patients.** (A) ETS1 level was detected to be correlated with NOTCH1 positively in breast cancer tissues. Staining intensity: 0 in case 1 (non-TNBC), 1 in case 2 (non-TNBC), 2 in case 3 (TNBC), 3 in case 4 (TNBC) (the magnification is 400 ×). (B–I) Using the PanCanSurvPlot database to evaluate the prognostic value (including OS, RFS and DMFS) of ETS1 and NOTCH1 in patients with breast cancer.

Table 4
Expression of ETS1 and NOTCH1 in breast cancer tissues.

Gene	Number	Low (%)	High (%)	χ2	*P*
ETS1	135	40 (29.63 %)	95 (70.37 %)	15.648	**0.000**
NOTCH1	135	14 (10.37 %)	121 (89.63 %)		

Table 5
Relationship between the expression of ETS1 and NOTCH1.

NOTCH1	ETS1				Spearman	*P*
	–	+	++	+++		
–	0	2	0	0	0.199	**0.021**
+	2	3	6	3		
++	5	6	20	6		
+++	1	15	44	22		

downstream genes. In esophageal squamous cell carcinoma, a series of downstream targets, including FERMT2, cMET, EGFR, PDK1, and survivin has been discovered for miR-338–5p duty in inhibiting proliferation, colony formation, migration, and cisplatin resistance, as well as promoting apoptosis and radiosensitivity [23,51–53]. In gastric cancer, miR-338–5p promotes the cisplatin resistance in malignant cells through targeting ZEB2, or facilities cancer progression via the LINC00240/miR-338–5p/METTL3 axis [24,54]. For glioma, miR-338–5p inhibits cancer progress of through targeting CTBP2, EFEMP1, FOXD1 and Hedgehog signals [21,55,56], yet Li et al. reported its promotion of glioma invasion via TSHZ3 and MMP2 regulation [57]. However, this study was limited to cellular experiments, necessitating additional data from animal and clinical studies for comprehensive validation. In colorectal cancer, many studies support the cancer-promoting contribution of miR-338–5p, promoting cancer metastatic progression by targeting PIK3C3 [25,58]. Conversely, it has been reported that *in vivo*, overexpression of miR-338–5p and the HIF-1α inhibitor PX-478 in colorectal cancer

cells can heighten oxaliplatin sensitivity by suppressing a feedback loop involving HIF-1α/miR-338–5p/IL-6, albeit under anoxic conditions [59]. We predicted the potential targeted genes of miR-338–5p through online databases. Previous experiments demonstrated that miR-338–5p inhibits NOTCH1 signaling in breast cancer cells. Interestingly, bioinformatic predictions did not suggest the direct rgulation of NOTCH1 by miR-338–5p. This suggests that miR-338–5p may regulate NOTCH1 expression through intermediary molecules or pathways. We continued to explore the transcription factors of NOTCH1, and found that ETS1 is not only a potential downstream molecule of miR-338–5p, but also one of the transcription factors that regulate NOTCH1 expression, which indicates that miR-338–5p may affect tumor progression by targeting the ETS1/NOTCH1 axis in breast cancer.

ETS1 is located on chromosome 11 and is expressed in various cell types, including endothelial cells, vascular smooth muscle cells, and epithelial cells [60]. Functioning as a transcriptional activator, ETS1 critically participates in stem cell development, cell senescence and death, and tumorigenesis. Elevated levels of ETS1 protein or mRNA expression are observed in several cancers, such as esophageal, breast, colorectal, hepatocellular, endometrial, gastric, and lung cancers, correlating with higher tumor grade, poor differentiation, increased tumor aggressiveness, and reduced patient survival [61–65]. Consistently in breast cancer, the level of ETS1 is predominantly found in TNBC, where it is associated with unfavorable patient outcomes [66]. Zhang et al. found that the proto-oncogene ETS1 was suppressed by miR-125 b, which is a tumor suppressor in human invasive breast cancer [67]. Additionally, miR-199–5p and miR-124 have been shown as upstream regulators for silence ETS1, which inhibits breast cancer development accordingly [68,69]. In astrocytoma, miR-338–5p was reported to target and regulate ETS1 expression for the first time [70]. Our study shows that miR-338–5p directly binds to the 3′UTR of ETS1. Moreover, miR-338–5p inhibits the proliferation, invasion and metastasis of breast cancers by silencing the expression of ETS1.

Previous studies have demonstrated that NOTCH1, NOTCH2, and NOTCH4 contribute to cancer promotion, whereas NOTCH3 exerts an inhibitory role in cancer progression [42,71]. This study shows that NOTCH1 is down-regulated in cells that overexpress miR-338–5p. However, bioinformatics failed to predict the potential combination between miR-338–5p and NOTCH1-3′UTR, so we postulated ETS1 was the link between miR-338–5p and NOTCH1. As a transcription factor, ETS1 combines with specific sequence in promoter of multiple targets to promote the transcription and expression of downstream genes. It is reported that ETS1 can bind to ZEB1 and ZEB2 promoters to activate their expression, thus promoting EMT in breast cancer [72,73]. Through chromatin immunoprecipitation, Bosman et al. discovered that alphaB-crystallin was the direct downstream target of ETS1 though binding to its promoter region in basal-like breast cancers [74]. Zhang et al. put forward the functional combination of ETS1 with IKKα promoter using luciferase detection and ChIP assays [75]. While ETS1 has been suggested to be a potential transcription factor for NOTCH1 in T-cell acute lymphoblastic leukemia, direct verification of this mechanism is lacking [76]. We show that ETS1 directly binds to the NOTCH1 promoter. Moreover, silencing ETS1 suppresses the malignant behavior of breast cancer cells through the down-regulation of NOTCH1. The positive correlation between ETS1 and NOTCH1 expression levels has been confirmed in cellular, animal, and clinical studies of breast cancer. Thus, miR-338–5p negatively regulates the ETS1/NOTCH1 axis and the progress of breast cancer by targeting the ETS1-3′UTR.

It is shown that the change of miRNA level is of great value in clinical application and gradually becomes a promising non-invasive biomarker and cancer treatment strategy. At present, based on molecular diagnosis technology, the detection of microRNA-25 for pancreatic cancer, microRNA-92a for colorectal cancer and MicroRNA-7™ for liver cancer has been carried out on the PCR platform, which continuously improves the sensitivity of cancer detection [77–79]. Current investigation indicates a significant down-regulation of miR-338–5p expression in breast cancer, particularly in TNBC, which arouses our attention to miR-338–5p as a new potential biomarker for predicting and diagnosing breast cancer and its prognosis. Currently, our research is confined to verification through cell and animal experiments and has not yet extended to clinical studies. Further research is essential to assess the role of miR-338–5p in clinical settings.

The further clinical application of miRNA for cancer treatment has always been the focus of research. Studies have demonstrated that miRNAs promoting cancer progression can be effectively suppressed using various approaches. These include anti-miRNA therapies, miRNA sponges, small molecule inhibitors (SMIRs), and CRISPR/Cas9-mediated knockout. Conversely, synthetic miRNA mimics or miRNA expression vectors can restore miRNA levels that have been inhibited [80–83]. However, these strategies exhibit greater efficacy *in vitro* compared to *in vivo* settings. Therefore, it is particularly important to explore a better delivery system. At present, microRNA delivery system based on nanoparticles has attracted the attention of pharmaceutical industry because of its small size, low molecular weight and high efficiency. MiR-34 is commonly down-regulated across various cancers and plays a critical regulatory role in tumor suppression. MRX34, a double-stranded RNA oligonucleotide, has been encapsulated in amphoteric liposomes and evaluated in diverse cancer types. Amphoteric liposomes prolong MRX34 circulation in the bloodstream and enhance its delivery to target tissues. In 2017, the initial phase I clinical trial in humans demonstrated that MRX34, in combination with dexamethasone, exhibited anti-tumor activity in patients with advanced solid tumors [84]. In addition, the virus-based microRNA delivery methods have emerged as promising tools for gene therapy due to their high transduction efficiency and sustained gene expression across various cell types [85]. For instance, the lentivirus-mediated overexpression of miR-145 has demonstrated efficacy in inhibiting the proliferation of esophageal cancer cells and inducing apoptosis [86]. Similarly, delivery of miR-124 and miR-145 mimics via mesenchymal stem cells has shown promise in reducing migration and self-renewal in glioma cells and glioma stem cells, both *in vitro* and *in vivo* [87]. Our research aims to explore the role and mechanism of miR-338–5p in inhibiting cancer metastasis in TNBC. Clinically, we aim to synthesize miR-338–5p mimics or expression vectors and explore effective delivery systems. This approach could offer novel strategies for breast cancer treatment, bridging promising preclinical research outcomes to potentially impactful clinical applications.

5. Conclusion

We explored the role of miR-338–5p in breast cancer and the molecular mechanism by which miR-338–5p regulates the ETS1/NOTCH1 axis in breast cancer. The aim is to contribute experimental insights into the mechanisms underlying breast cancer invasion and metastasis, offering potential therapeutic strategies and treatment targets for clinical research and development.

Data availability statement

The data supporting the findings in current investigation are available upon reasonable request.

Funding

This investigation was supported by the National Natural Science Foundation of China (No. 82273457 and 81501539), Special Grant for Key Area Programs of Guangdong Education Department, China (No. 2021ZDZX2040), the Guangdong Basic and Applied Basic Research Foundation, China (No. 2023A1515012762), Science and Technology Special Project of Guangdong Province, China (No. 210715216902829), and 'Dengfeng Project' for the construction of high-level hospitals in Guangdong Province—First Affiliated Hospital of Shantou University College Supporting Funding, China (No. 202003–10).

CRediT authorship contribution statement

Wen-Jia Chen: Conceptualization, Data curation, Methodology, Visualization, Writing – original draft. **Qian-Qian Ye:** Conceptualization, Data curation, Methodology, Visualization, Writing – original draft. **Hua-Tao Wu:** Conceptualization, Data curation, Methodology, Visualization, Writing – original draft. **Zheng Wu:** Formal analysis, Investigation. **Yang-Zheng Lan:** Project administration, Resources. **Ze-Xuan Fang:** Software. **Wen-Ting Lin:** Validation. **Jing Liu:** Conceptualization, Data curation, Funding acquisition, Methodology, Supervision, Writing – review & editing.

Declaration of competing interest

The authors declare that they have no known competing financial interests or personal relationships that could have appeared to influence the work reported in this paper.

References

[1] R.L. Siegel, et al., Cancer statistics, 2023, Ca - Cancer J. Clin. 73 (1) (2023) 17–48.
[2] L. Wilkinson, T. Gathani, Understanding breast cancer as a global health concern, Br. J. Radiol. 95 (1130) (2022) 20211033.
[3] R. Dent, et al., Triple-negative breast cancer: clinical features and patterns of recurrence, Clin. Cancer Res. 13 (15 Pt 1) (2007) 4429–4434.
[4] P. Ferrari, et al., Molecular mechanisms, biomarkers and emerging therapies for chemotherapy resistant TNBC, Int. J. Mol. Sci. 23 (3) (2022).
[5] D. Neelakantan, et al., EMT cells increase breast cancer metastasis via paracrine GLI activation in neighbouring tumour cells, Nat. Commun. 8 (2017) 15773.
[6] I. Pastushenko, C. Blanpain, EMT transition states during tumor progression and metastasis, Trends Cell Biol. 29 (3) (2019) 212–226.
[7] J.P. Thiery, et al., Epithelial-mesenchymal transitions in development and disease, Cell 139 (5) (2009) 871–890.
[8] S. Elzamly, et al., Epithelial-mesenchymal transition markers in breast cancer and pathological responseafter neoadjuvant chemotherapy, Breast Cancer 12 (2018) 1178223418788074.
[9] S. Shao, et al., Notch1 signaling regulates the epithelial-mesenchymal transition and invasion of breast cancer in a Slug-dependent manner, Mol. Cancer 14 (1) (2015) 28.
[10] M. Saitoh, Epithelial-mesenchymal transition is regulated at post-transcriptional levels by transforming growth factor-beta signaling during tumor progression, Cancer Sci. 106 (5) (2015) 481–488.
[11] H. Jiang, et al., Jagged1-Notch1-deployed tumor perivascular niche promotes breast cancer stem cell phenotype through Zeb1, Nat. Commun. 11 (1) (2020) 5129.
[12] J. Chen, et al., Hypoxia potentiates Notch signaling in breast cancer leading to decreased E-cadherin expression and increased cell migration and invasion, Br. J. Cancer 102 (2) (2010) 351–360.
[13] C. Sahlgren, et al., Notch signaling mediates hypoxia-induced tumor cell migration and invasion, Proc. Natl. Acad. Sci. U. S. A. 105 (17) (2008) 6392–6397.
[14] L. He, G.J. Hannon, MicroRNAs: small RNAs with a big role in gene regulation, Nat. Rev. Genet. 5 (7) (2004) 522–531.
[15] R.S. Pillai, MicroRNA function: multiple mechanisms for a tiny RNA? RNA 11 (12) (2005) 1753–1761.
[16] J.P. Munoz, et al., The role of MicroRNAs in breast cancer and the challenges of their clinical application, Diagnostics 13 (19) (2023).
[17] S. Paszek, et al., Dysregulation of microRNAs in triple-negative breast cancer, Ginekol. Pol. 88 (10) (2017) 530–536.
[18] S. Barik, An intronic microRNA silences genes that are functionally antagonistic to its host gene, Nucleic Acids Res. 36 (16) (2008) 5232–5241.
[19] D. Montenegro, et al., Differential expression of microRNAs with progression of gestation and inflammation in the human chorioamniotic membranes, Am. J. Obstet. Gynecol. 197 (3) (2007) 289 e1–e6.
[20] X. Zhao, et al., MicroRNA-mediated control of oligodendrocyte differentiation, Neuron 65 (5) (2010) 612–626.
[21] D.Z. Liu, et al., MiR-338 suppresses cell proliferation and invasion by targeting CTBP2 in glioma, Cancer Biomarkers 20 (3) (2017) 289–297.
[22] H. Zhou, et al., Chidamide inhibits glioma cells by increasing oxidative stress via the miRNA-338-5p regulation of Hedgehog signaling, Oxid. Med. Cell. Longev. 2020 (2020) 7126976.
[23] W.C. Lin, et al., miR-338-5p inhibits cell proliferation, colony formation, migration and cisplatin resistance in esophageal squamous cancer cells by targeting FERMT2, Carcinogenesis 40 (7) (2019) 883–892.
[24] X. Wei, et al., miR-338-5p-ZEB2 axis in diagnostic, therapeutic predictive and prognostic value of gastric cancer, J. Cancer 12 (22) (2021) 6756–6772.
[25] E. Bilegsaikhan, et al., Circulating miR-338-5p is a potential diagnostic biomarker in colorectal cancer, J Dig Dis 19 (7) (2018) 404–410.
[26] H. Wu, F. Li, R. Zhu, miR-338-5p inhibits cell growth and migration via inhibition of the METTL3/m6A/c-Myc pathway in lung cancer, Acta Biochim. Biophys. Sin. 53 (3) (2021) 304–316.
[27] J. Sun, L. Chen, M. Dong, MiR-338-5p inhibits EGF-induced EMT in pancreatic cancer cells by targeting EGFR/ERK signaling, Front. Oncol. 11 (2021) 616481.

[28] Y. Chen, et al., Plasma miR-15b-5p, miR-338-5p, and miR-764 as biomarkers for hepatocellular carcinoma, Med. Sci. Mon. Int. Med. J. Exp. Clin. Res. 21 (2015) 1864–1871.
[29] R. Edgar, M. Domrachev, A.E. Lash, Gene Expression Omnibus: NCBI gene expression and hybridization array data repository, Nucleic Acids Res. 30 (1) (2002) 207–210.
[30] F. Biagioni, et al., miR-10b*, a master inhibitor of the cell cycle, is down-regulated in human breast tumours, EMBO Mol. Med. 4 (11) (2012) 1214–1229.
[31] R. Li, et al., CancerMIRNome: an interactive analysis and visualization database for miRNome profiles of human cancer, Nucleic Acids Res. 50 (D1) (2022) D1139–D1146.
[32] J.H. Li, et al., starBase v2.0: decoding miRNA-ceRNA, miRNA-ncRNA and protein-RNA interaction networks from large-scale CLIP-Seq data, Nucleic Acids Res. 42 (Database issue) (2014) D92–D97.
[33] N. Matamala, et al., Tumor microRNA expression profiling identifies circulating microRNAs for early breast cancer detection, Clin. Chem. 61 (8) (2015) 1098–1106.
[34] Y. Chen, X. Wang, miRDB: an online database for prediction of functional microRNA targets, Nucleic Acids Res. 48 (D1) (2020) D127–D131.
[35] I. Kavakiotis, et al., DIANA-miTED: a microRNA tissue expression database, Nucleic Acids Res. 50 (D1) (2022) D1055–D1061.
[36] Q. Zhang, et al., hTFtarget: a comprehensive database for regulations of human transcription factors and their targets, Dev. Reprod. Biol. 18 (2) (2020) 120–128.
[37] I. Rauluseviciute, et al., Jaspar 2024: 20th anniversary of the open-access database of transcription factor binding profiles, Nucleic Acids Res. (2023).
[38] I. de Bruijn, et al., Analysis and visualization of longitudinal genomic and clinical data from the AACR Project GENIE biopharma collaborative in cBioPortal, Cancer Res. 83 (23) (2023) 3861–3867.
[39] Z. Hu, et al., The molecular portraits of breast tumors are conserved across microarray platforms, BMC Genom. 7 (2006) 96.
[40] J.S. Parker, et al., Supervised risk predictor of breast cancer based on intrinsic subtypes, J. Clin. Oncol. 27 (8) (2009) 1160–1167.
[41] M. Callari, et al., Subtype-dependent prognostic relevance of an interferon-induced pathway metagene in node-negative breast cancer, Mol. Oncol. 8 (7) (2014) 1278–1289.
[42] J. Liu, et al., Targeting Notch degradation system provides promise for breast cancer therapeutics, Crit. Rev. Oncol. Hematol. 104 (2016) 21–29.
[43] Y.S. Xiao, et al., Major vault protein is a direct target of Notch1 signaling and contributes to chemoresistance in triple-negative breast cancer cells, Cancer Lett. 440–441 (2019) 156–167.
[44] Y. Qi, et al., Notch1 promotes resistance to cisplatin by up-regulating Ecto-5'-nucleotidase (CD73) in triple-negative breast cancer cells, Cell Death Dis. 9 (1) (2023) 204.
[45] X.Y. Niu, Z.Q. Zhang, P.L. Ma, MiRNA-221-5p promotes breast cancer progression by regulating E-cadherin expression, Eur. Rev. Med. Pharmacol. Sci. 23 (16) (2019) 6983–6990.
[46] Y. Lu, et al., MicroRNA-140-5p inhibits invasion and angiogenesis through targeting VEGF-A in breast cancer, Cancer Gene Ther. 24 (9) (2017) 386–392.
[47] F. Zhang, et al., Methylation of microRNA-338-5p by EED promotes METTL3-mediated translation of oncogene CDCP1 in gastric cancer, Aging (Albany NY) 13 (8) (2021) 12224–12238.
[48] V. Bhatia, et al., Epigenetic silencing of miRNA-338-5p and miRNA-421 drives SPINK1-positive prostate cancer, Clin. Cancer Res. 25 (9) (2019) 2755–2768.
[49] J. Long, J. Luo, X. Yin, MiR-338-5p promotes the growth and metastasis of malignant melanoma cells via targeting CD82, Biomed. Pharmacother. 102 (2018) 1195–1202.
[50] L. Xu, et al., LncRNA MBLN1-AS1 inhibits the progression of retinoblastoma through targeting miR-338-5p-Wnt/beta-catenin signaling pathway, Inflamm. Res. 70 (2) (2021) 217–227.
[51] D. Cui, et al., Dual inhibition of cMET and EGFR by microRNA-338-5p suppresses metastasis of esophageal squamous cell carcinoma, Carcinogenesis 42 (7) (2021) 995–1007.
[52] M. Park, et al., MiR-338-5p enhances the radiosensitivity of esophageal squamous cell carcinoma by inducing apoptosis through targeting survivin, Sci. Rep. 7 (1) (2017) 10932.
[53] J. Wang, et al., Circ_0001944 depletion inhibits glycolysis and esophageal cancer progression by binding to miR-338-5p to reduce PDK1 expression, J. Bioenerg. Biomembr. (2023).
[54] G. Wang, Z. Zhang, C. Xia, Long non-coding RNA LINC00240 promotes gastric cancer progression via modulating miR-338-5p/METTL3 axis, Bioengineered 12 (2) (2021) 9678–9691.
[55] D. Lei, et al., MiR-338-5p suppresses proliferation, migration, invasion, and promote apoptosis of glioblastoma cells by directly targeting EFEMP1, Biomed. Pharmacother. 89 (2017) 957–965.
[56] Q. Ma, T. Yang, E2F transcription factor 1/small nucleolar RNA host gene 18/microRNA-338-5p/forkhead box D1: an important regulatory axis in glioma progression, Bioengineered 13 (1) (2022) 418–430.
[57] Y. Li, et al., MiR-338-5p promotes glioma cell invasion by regulating TSHZ3 and MMP2, Cell. Mol. Neurobiol. 38 (3) (2018) 669–677.
[58] C.A. Chu, et al., MiR-338-5p promotes metastasis of colorectal cancer by inhibition of phosphatidylinositol 3-kinase, catalytic subunit type 3-mediated autophagy pathway, EBioMedicine 43 (2019) 270–281.
[59] K. Xu, et al., Hypoxia induces drug resistance in colorectal cancer through the HIF-1alpha/miR-338-5p/IL-6 feedback loop, Mol. Ther. 27 (10) (2019) 1810–1824.
[60] D.W. Lincoln 2nd, K. Bove, The transcription factor Ets-1 in breast cancer, Front. Biosci. 10 (2005) 506–511.
[61] N. Takai, et al., Expression of c-Ets1 is associated with malignant potential in endometrial carcinoma, Cancer 89 (10) (2000) 2059–2067.
[62] T. Nakayama, et al., Expression of the Ets-1 proto-oncogene in human gastric carcinoma: correlation with tumor invasion, Am. J. Pathol. 149 (6) (1996) 1931–1939.
[63] T. Nakayama, et al., Expression of the ets-1 proto-oncogene in human colorectal carcinoma, Mod. Pathol. 14 (5) (2001) 415–422.
[64] I. Takanami, K. Takeuchi, M. Karuke, Expression of ETS-1 is correlated with urokinase-type plasminogen activator and poor prognosis in pulmonary adenocarcinoma, Tumour Biol 22 (4) (2001) 205–210.
[65] K. Kanda, et al., Expression of the Ets-1 proto-oncogene is linked to cell differentiation of human hepatocellular carcinoma, Hepato-Gastroenterology 49 (45) (2002) 747–751.
[66] E. Charafe-Jauffret, et al., Gene expression profiling of breast cell lines identifies potential new basal markers, Oncogene 25 (15) (2006) 2273–2284.
[67] Y. Zhang, et al., miR-125b is methylated and functions as a tumor suppressor by regulating the ETS1 proto-oncogene in human invasive breast cancer, Cancer Res. 71 (10) (2011) 3552–3562.
[68] W. Li, et al., miR-199a-5p regulates β1 integrin through Ets-1 to suppress invasion in breast cancer, Cancer Sci. 107 (7) (2016) 916–923.
[69] W. Li, et al., MicroRNA-124 inhibits cellular proliferation and invasion by targeting Ets-1 in breast cancer, Tumour Biol 35 (11) (2014) 10897–10904.
[70] J. Wang, et al., Hypermethylation of the promoter of miR-338-5p mediates aberrant expression of ETS-1 and is correlated with disease severity of astrocytoma patients, Front. Oncol. 11 (2021) 773644.
[71] Y. Wu, et al., MicroRNA-488 inhibits proliferation and motility of tumor cells via downregulating FSCN1, modulated by Notch3 in breast carcinomas, Cell Death Dis. 11 (10) (2020) 912.
[72] A. Furlan, et al., Ets-1 triggers and orchestrates the malignant phenotype of mammary cancer cells within their matrix environment, J. Cell. Physiol. 215 (3) (2008) 782–793.
[73] Y.H. Park, et al., Ets-1 upregulates HER2-induced MMP-1 expression in breast cancer cells, Biochem. Biophys. Res. Commun. 377 (2) (2008) 389–394.
[74] J.D. Bosman, et al., Regulation of alphaB-crystallin gene expression by the transcription factor Ets1 in breast cancer, Breast Cancer Res. Treat. 119 (1) (2010) 63–70.
[75] Y. Zhang, et al., ETS1 is associated with cisplatin resistance through IKKalpha/NF-kappaB pathway in cell line MDA-MB-231, Cancer Cell Int. 18 (2018) 86.
[76] A.C. McCarter, et al., Combinatorial ETS1-dependent control of oncogenic NOTCH1 enhancers in T-cell leukemia, Blood Cancer Discov 1 (2) (2020) 178–197.

[77] J. Zhang, et al., Excessive miR-25-3p maturation via N(6)-methyladenosine stimulated by cigarette smoke promotes pancreatic cancer progression, Nat. Commun. 10 (1) (2019) 1858.
[78] N. Yamada, et al., Role of intracellular and extracellular MicroRNA-92a in colorectal cancer, Transl Oncol 6 (4) (2013) 482–492.
[79] D.T. Chu, et al., Recent progress of stem cell therapy in cancer treatment: molecular mechanisms and potential applications, Cells 9 (3) (2020).
[80] D. Bhere, et al., Simultaneous downregulation of miR-21 and upregulation of miR-7 has anti-tumor efficacy, Sci. Rep. 10 (1) (2020) 1779.
[81] M.F. Corsten, et al., MicroRNA-21 knockdown disrupts glioma growth in vivo and displays synergistic cytotoxicity with neural precursor cell delivered S-TRAIL in human gliomas, Cancer Res. 67 (19) (2007) 8994–9000.
[82] J.F. Lima, et al., Anti-miRNA oligonucleotides: a comprehensive guide for design, RNA Biol. 15 (3) (2018) 338–352.
[83] G. Aquino-Jarquin, Emerging role of CRISPR/Cas9 technology for MicroRNAs editing in cancer research, Cancer Res. 77 (24) (2017) 6812–6817.
[84] M.S. Beg, et al., Phase I study of MRX34, a liposomal miR-34a mimic, administered twice weekly in patients with advanced solid tumors, Invest. N. Drugs 35 (2) (2017) 180–188.
[85] Y. Chen, D.Y. Gao, L. Huang, In vivo delivery of miRNAs for cancer therapy: challenges and strategies, Adv. Drug Deliv. Rev. 81 (2015) 128–141.
[86] J.H. Zhang, et al., Episomal lentiviral vector-mediated miR-145 overexpression inhibits proliferation and induces apoptosis of human esophageal carcinomas cells, Recent Pat. Anti-Cancer Drug Discov. 11 (4) (2016) 453–460.
[87] H.K. Lee, et al., Mesenchymal stem cells deliver synthetic microRNA mimics to glioma cells and glioma stem cells and inhibit their cell migration and self-renewal, Oncotarget 4 (2) (2013) 346–361.